Optimized synergetic control approach for a six-phase asynchronous generator coupled to an intelligent flywheel energy storage system

Djamel DERKOUCHE, Katia KOUZI

University Amar Telidji of Laghouat, Algeria
Semiconductors and Functional Materials Laboratory

derkouche@gmail.com, k.kouzi@lagh-univ.dz

Abstract: This paper seeks to improve the efficiency of a whole wind power conversion system (WPCS) based on a dual star asynchronous machine (DSAM) incorporated with a flywheel energy storage system (FESS) based on an induction machine (IM). The FESS is connected to the wind generator through the DC bus link in order to control the amount of power delivered to the analysed network. The FESS has gained a lot of attention recently because of its low costs, long lifetime, and clean technology. This paper proposes a powerful control strategy based on a synergetic approach with a vector control applied to the DSAM and a Fuzzy logic controller applied to the FESS machine, this control can ensure a quick response time and a good stability of the system over the whole operating range, and can guarantee system robustness. Moreover, the Particle Swarm Optimization algorithm is proposed for fixing the problem of synergetic controller parameter tuning, which enhances the effectiveness of the control system. The dynamic model of the suggested system of the wind power generator is simulated in Matlab/Simulink for all points of operation. The obtained results which are presented and discussed in this paper, show how well the proposed model worked.

Keywords: Dual star induction machine, Induction machine, Synergetic controller, Vector control, Flywheel enegy storage system, Fuzzy controller, PSO Algorithm.

1. Introduction

The best thing that could be done to lessen the effects of pollution and climate change on health is to use green energy, such as wind and solar power. Additionally, the need for energy globally is rising quickly and the transition to renewable energy sources is more than necessary. The wind is one of the most significant sources of renewable energy, and it has recently become more popular as a source of electricity. Variable-speed wind energy conversion systems (VSWECS) have several advantages over fixed-speed systems, including higher energy capture capabilities, improved efficiency, and power quality by employing Maximum Power Point Tracking. Multi-phase machines have various advantages over three-phase ones they might be a good candidate for a variable speed drive control, the same stator contains all of their windings. A known example of the aforementioned devices is the dual star asynchronous machine (DSAM), which has numerous benefits, including segmented power, good stability, and a decrease in torque waves (Chen & Fang, 2003).

It can be agreed that the nature of the wind is random, so the turbines produce fluctuating power; this is a major obstacle in the production, storage, and distribution of this energy. Energy storage systems (ESSs) could become a key component of smart grids in the future and could play a critical role in solving this problem. If energy production from distributed generation sources is not generating as much electricity as anticipated, the microgrid in grid-connected mode can be used to augment the power. There are many different types of ESSs and they can be divided into two groups. (Cimuca, 2005); The first group involves energy storing for a long time, in which the storage lasts for more than 10 minutes such as battery energy storage systems. The second group involves energy storing for a short time where the storage time is under 10 minutes, and it includes electrical double-layer capacitors (EDLCs), superconducting magnet (SM) systems, and Flywheel Energy Storage Systems (FESSs). The latter have garnered a great deal of interest recently because of their low costs, long lifetime, and quick response. The crucial task of FESSs is to help the wind turbines contribute to the grid and improve the quality of produced electric power. In contrast to environmentally hazardous battery storage methods, FESS is a clean technology that does not hurt the environment. Transforming the kinetic energy in the flywheel into electric power is the basic idea behind FESS,

https://doi.org/10.33436/v32i4y202209

which consists of three main components: the flywheel, the electrical machine, and the electronic power converters. FESS efficiency depends on the type of the machine employed, various types of electrical machines have been applied FESS, among these there are three main types of machines: Firstly, switched reluctance machines (SRM) which have a low power factor, are noisy and require expensive power electronics. Secondly, Permanent-Magnet Synchronous machines (PMSM) are often more expensive and more susceptible to temperature changes, with the risk of demagnetization. Finally, induction machines (IMs) are utilized for high-power applications due to their rugged construction (Mousavi et al., 2017). However, the control design of WECSs is becoming more difficult due to the linear dynamics like the changing of the parameters of the machine such as rotor resistance due to a short-circuit. Conventional regulator control has been largely used in industry, it is based on proportional-integral (PI) regulators, PI control is a simple implementation and uses the state model with constant coefficients. Nevertheless, it requires adjustment and is weak in the face of changing parameters. Therefore, many studies have been carried out to find a solution to this problem by using non-linear ordering techniques, which are frequently used and have demonstrated efficiency in a variety of applications due to their simplicity, fast response speed, and robustness. Among these ordering techniques there is the Sliding Mode Control (SMC), which depends on modifying the control structure in response to the system conditions and ensures that it runs with a good performance. Although this approach is interesting, it affected by a big problem called the chattering phenomenon, this keeps the system from sliding over the reference surface and instead leads the system to oscillating around it, which in turn affects the control of the machine, and causes a big problem.

For reducing the chattering phenomenon, a novel control technique was employed for regulating nonlinear systems, it was proposed by (Kolesnikov et al., 2000) it is called the Synergetic Approach to Control Theory (SACT) and involves using the macro variables and their derivative in the first moment to achieve zero variation in a given span of time. During the control process, SACT cancels the non-linearity of the system, thus facilitating the control process. Numerous studies have been carried out on the control of electrical drives by using the synergetic control (SC) due to its primary attributes of beautiful interface and simple construction. (Davoudi et al., 2008; Guermit & Kouzi, 2018). In the area of electrical machinery control, SACT has been investigated and established itself as a valuable member of the robust control community and is becoming an alternative approach to the sliding mode.

However, there are parameters that are not optimal which must be set up in the synergetic control, incorrect settings can result in control with a long settling time or overshoot, which is unacceptable. The best way to choose the proper settings for any control system is using optimization methods such as ACO, GA, BFO, and PSO. The last one is a powerful optimization method that gives optimal parameters for obtaining a high performance for the proposed control approach. The PSO is one of the contemporary optimization techniques that can be used to solve nonlinear optimization issues, it has been introduced by (Kennedy & Eberhart, 1995). PSO has a number of advantages, including the capacity to improve without depending on objective function evaluation, quick implementation time, and simple computer execution.

Various FESSs techniques (Davigny, 2007; Cimuca et al., 2010 and Amimeur, 2012) have been developed for integrating the WPCS into the electrical grid in order to maintain the balance between production and consumption by using the flywheel energy storage due to its benefits in improving the electric power quality (Jia et al., 2022). This research focuses on the integration of a fuzzy FESS based on the induction machine with an optimized synergetic approach of DSAG by PSO algorithm. The special merit of the induction machines lies in the fact that they are robust, require little maintenance, have no supply to magnetize them and are low-cost.

In this article, our goal is to model and simulate a wind turbine based on a squirrel cage asynchronous machine associated with a storage unit FESS to maintain the power produced as constant as possible. A wind turbine, gearbox, a dual star asynchronous generator, four converters, a transformer, an input filter, and the FESS which itself is made up of a flywheel and an induction machine, are all depicted in the general representation of the analyzed control system in Figure 1.

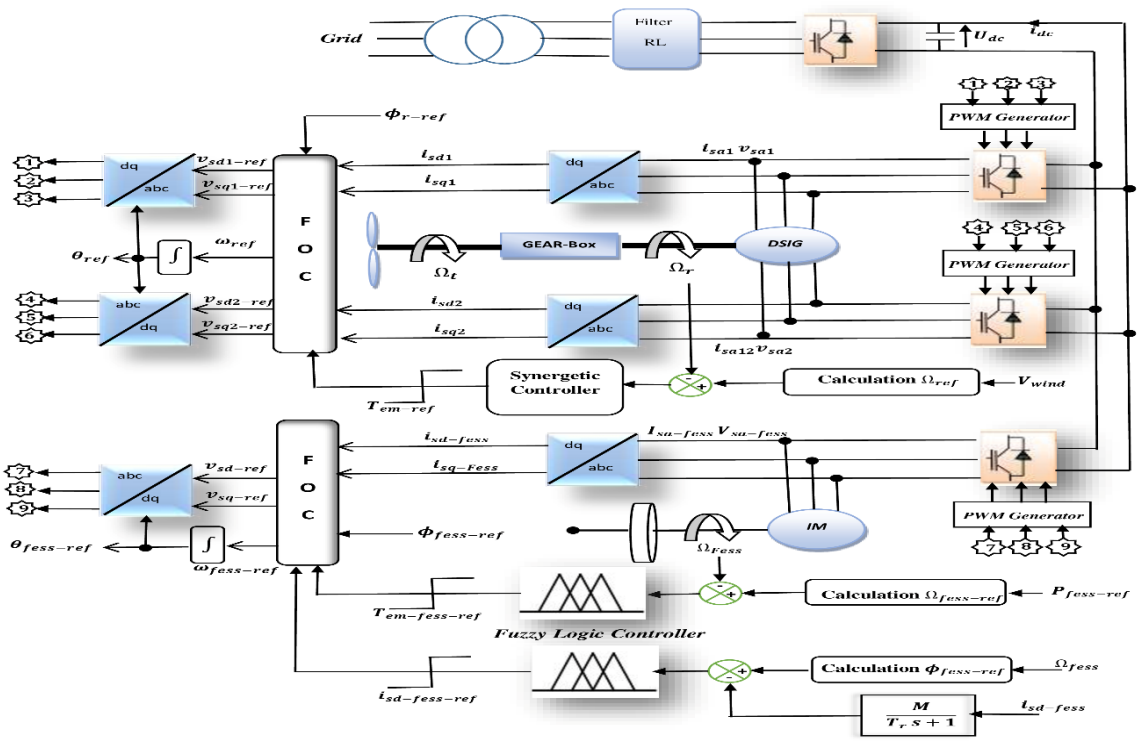

Figure 1. Block diagram of the control system (Amimeur, 2012)

The paper is organized as follows, Section 1 presents the introduction. The modeling of the complete system is presented in Section 2. Sections 3 and 4 present the vector control of DSAG and IM and the synergetic control of DSAG, respectively. The particle swarm optimization is presented in Section 5, while Section 6 describes in detail the fuzzy design of the flywheel energy storage unit. The results are discussed in Section 7. Finally, the conclusion is in Section 8.

2. The complete system mathematical model

2.1. Wind turbine model

The power of the turbine P_t, which passes the surface equivalent to the active surface S of the turbine, can be calculated from the kinetic energy of the movement of air mass passing through the area of surface S of the blade. (Gergaud et al., 2001; Hamidat et al., 2022):

$$P_t = C_p(\lambda)\rho SV^3/2 \tag{1}$$

where: C_p is the power coefficient, ρ is the density of air (kg/m^3), and V is the speed of the wind (m/s).

The number of rotor blades as well as their geometric and aerodynamic forms affect the power coefficient C_p, they are produced using required rated power, and regulatory type attributes. A gearbox with a gear ratio G, controls the speed of the generator shaft, which connects the turbine to the generator shaft. The term λ which represents "reduced speed" is used to refer to the ratio between the linear speed at the turbine blade and the wind speed, and it is used to characterize the operating speed of the wind turbines (El Aimani, 2004;):

$$T_G = \frac{T_t}{G},\ \Omega_t = \frac{\Omega_r}{G}, \text{ and } \lambda = \frac{\Omega_t R}{V} \tag{2}$$

where: T_G is the generator torque, T_t is the turbine torque, Ω_t is the turbine speed, and Ω_r is the mechanical speed of the generator.

As it is shown in Figure 2, a synergetic control of the rotation speed allows for the maximum value of the ratio between the power extracted and that of the wind and allows for maximum power point (MPP) extraction despite frequent variations in the wind speed, to keep the power coefficient percent at its highest level.

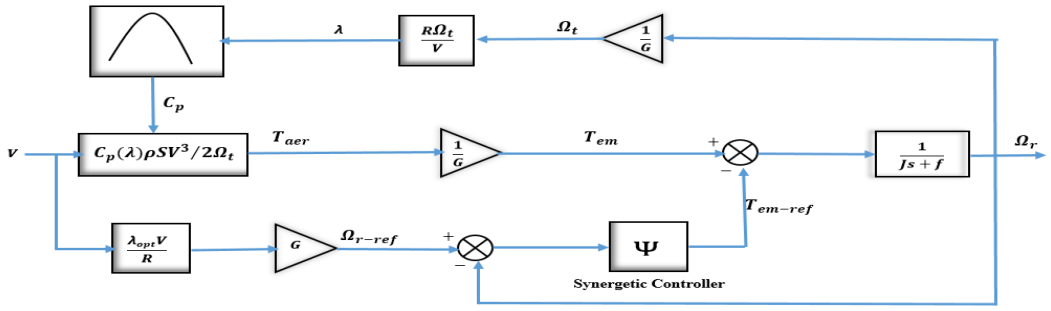

Figure 2. Block diagram of the turbine with maximization of the extracted power using a synergetic speed controller

The wind torque can be determined as follows

$$T_t = \frac{P_t}{\Omega_t} = C_p(\lambda)\rho SV^3/2\Omega_t \tag{3}$$

2.2. Model of the dual star asynchronous machine

Figure 3 shows a representation of the rotor and stator windings of a dual star asynchronous machine. Three phases are distributed in each winding of the dual star induction machine, and their magnetic axes are 120 degrees apart. The following system (4) provides the DSAM electrical models. (Amimeur et al., 2012):

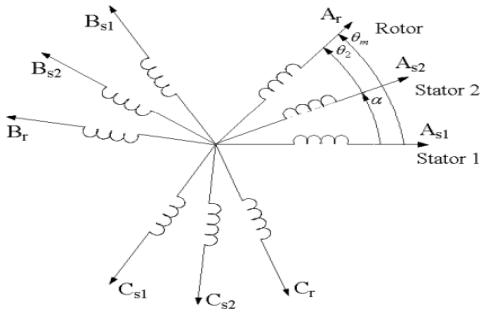

Figure 3. Vector representation of DSAG

$$\dot{X} = AX + BU \tag{4}$$

$$A = \begin{pmatrix} \frac{l_a - l_{s1}}{T_{s1}l_{s1}} & \omega_s & \frac{l_a}{T_{s1}l_{s2}} & 0 & \frac{l_a}{T_{s1}l_r} & 0 \\ -\omega_s & \frac{l_a - l_{s1}}{T_{s1}l_{s1}} & 0 & \frac{l_a}{T_{s1}l_{s2}} & 0 & \frac{l_a}{T_{s1}l_r} \\ \frac{l_a}{T_{s2}l_{s1}} & 0 & \frac{l_a - l_2}{T_{s2}l_{s2}} & \omega_s & \frac{l_a}{T_{s2}l_r} & 0 \\ 0 & \frac{l_a}{T_{s2}l_{s1}} & -\omega_s & \frac{l_a - l_2}{T_{s2}l_{s2}} & 0 & \frac{l_a}{T_{s2}l_r} \\ \frac{l_a}{T_r l_{s1}} & 0 & \frac{l_a}{T_r l_{s2}} & 0 & \frac{l_a - l_r}{T_r l_r} & \omega_{gl} \\ 0 & \frac{l_a}{T_r l_{s1}} & 0 & \frac{l_a}{T_r l_{s2}} & -\omega_{gl} & \frac{l_a - l_r}{T_r l_r} \end{pmatrix}, \quad B = \begin{pmatrix} 1 & 0 & 0 & 0 & 0 & 0 \\ 0 & 1 & 0 & 0 & 0 & 0 \\ 0 & 0 & 1 & 0 & 0 & 0 \\ 0 & 0 & 0 & 1 & 0 & 0 \\ 0 & 0 & 0 & 0 & 0 & 0 \\ 0 & 0 & 0 & 0 & 0 & 0 \end{pmatrix}$$

with $l_a = 1/\left(\frac{1}{l_{s1}} + \frac{1}{l_{s2}} + \frac{1}{l_r} + \frac{1}{l_m}\right)$, $T_{s1} = l_{s1}/r_{s1}$, $T_{s2} = l_{s2}/r_{s2}$ and $T_r = l_r/r_r$

$$X = \left[\phi_{sd1}\phi_{sq1}\phi_{sd2}\phi_{sq2}\phi_{rd}\phi_{rq}\right]^T, \quad U = \left[v_{sd1}v_{sq1}v_{sd2}v_{sq2}00\right]^T$$

The dynamic equation is as follows

$$J\frac{d\Omega_r}{dt} = T_{em} - T_L - k_f\Omega_r \tag{5}$$

where: $\frac{d\Omega_r}{dt}$ is the derivative of the mechanical speed with the respect to time.

2.3. Model of the FESS

Due to the variations in the wind speed, the power supplied by a wind generator is always variable, the energy flywheel storage unit is an excellent way to integrate the wind turbines into the ancillary services and produce a constant power. Figure 4 shows the control principle of the FESS integrated into the wind turbine. Knowing the energy that has to be transferred to the network or to the isolated loads P_{reg} and the energy generated by the wind turbine generator P_{ge}, the reference power of the FESS can be found by the following equation (Leclerq, 2004):

$$P_{fess-ref} = P_{reg} - P_{ge} \tag{6}$$

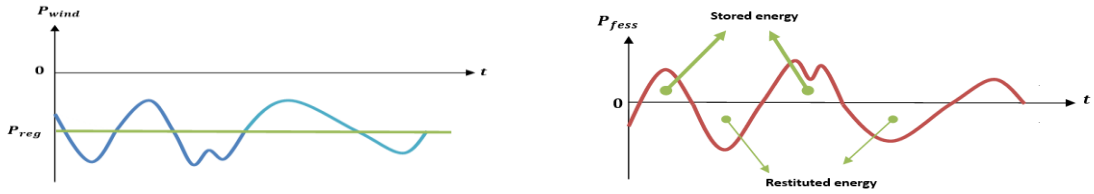

Figure 4. FESS working principle

2.3.1. Flywheel model

The kinetic energy stored by the flywheel is obtained by

$$E_c = \frac{1}{2}J_{fess}\Omega_{fess}^2 \tag{7}$$

where Ω_{fess} is the mechanical speed of the flywheel.

The reference of the energy stored in the flywheel can be obtained as follows (Cimuca, 2005):

$$E_{c-ref} = E_c^{t0} + \int_{t0}^{t1} P_{fess-ref}\,dt \tag{8}$$

where: E_c^{t0} represents the flywheel initial energy.

The dynamic equation of electric machine of the Fess is given by

$$J_{fess}\frac{d\Omega_{fess}}{dt} = T_{em-fess} - f_{fess}\Omega_{fess} - T_L \tag{9}$$

Replacing equation (7) in (8), the flywheel reference velocity is determined as

$$\Omega_{fess-ref} = \sqrt{\frac{2E_{c-ref}}{J_{fess}}} \tag{10}$$

Figure 5 represents the power and the torque of an asynchronous machine as a function of the speed.

- For $0 \le \Omega_{fess} \le \Omega_{rated}$, the rated torque is accessible in this zone, but the power is less than nominal, rises with speed, and eventually achieves the rated value at a base speed.
- For $\Omega_{rated} \le \Omega_{fess} \le 2\Omega_{rated}$, in this zone, the torque decreases in such a way as to keep the machine power at its rated level, this is the operating zone used in the FESS.

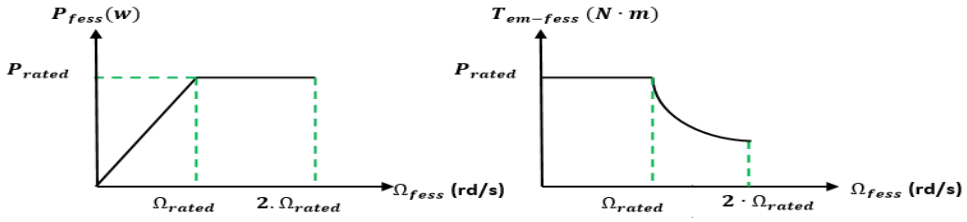

Figure 5. Torque and power of the FESS a function of the speed

The inertial moment can be obtained by

$$J_{fess} = \frac{P_{fess}\Delta t}{(\Omega_{fess-\max}^2 - \Omega_{fess-\min}^2)} \tag{11}$$

where Δt is the difference of time between the charge and discharge cycle [s], and P_{fess} is the power of the FESS machine.

2.3.2. Induction machine model

The park model makes it possible to conserve power when switching from the three-phase system to the two-phase system as follows (Davigny, 2007):

$$\frac{d}{dt}\begin{pmatrix}\phi_{rd-fess}\\ \phi_{rq-fess}\\ i_{sd-fess}\\ i_{sq-fess}\end{pmatrix} = \begin{pmatrix} \frac{-R_r}{L_r} & (\omega_{fess} - p\Omega_{fess}) & \frac{MR_r}{L_r} & 0 \\ (\omega_{fess} - p\Omega_{fess}) & \frac{-R_r}{L_r} & 0 & \frac{MR_r}{L_r} \\ \frac{MR_r}{\sigma L_s L_r^2} & \frac{Mp\Omega_{fess}}{\sigma L_s L_r} & \frac{-R_{sr}}{\sigma L_s} & \omega_{fess} \\ \frac{-Mp\Omega_{fess}}{\sigma L_s L_r} & \frac{MR_r}{\sigma L_s L_r^2} & -\omega_{fess} & \frac{-R_{sr}}{\sigma L_s} \end{pmatrix}\begin{pmatrix}\phi_{rd-fess}\\ \phi_{rq-fess}\\ i_{sd-fess}\\ i_{sq-fess}\end{pmatrix} + \begin{pmatrix} 0 & 0 \\ 0 & 0 \\ \frac{1}{\sigma L_s} & 0 \\ 0 & \frac{1}{\sigma L_s} \end{pmatrix}\begin{pmatrix} v_{rd-fess} \\ v_{rq-fess} \\ 0 \\ 0 \end{pmatrix} \tag{12}$$

with: $R_{sr} = R_s + (M^2 R_r / L_r^2)$ and $\sigma = 1 - (M^2 / L_s L_r)$

3. Flux-oriented control of DSAG and IM

The vector control method is based on the fact of introducing a control law that results in torque adjustment properties resembling those of a DC electrical machine and independent excitation by directing one of the flux components of the air gap, rotor, or stator on an axis of the reference frame rotating at the speed. Induction machines controlled by flux orientation involve controlling the flux with one component of the current and the torque with the other component. In this work, the orientation of the rotor flux is chosen so $\phi_{rd} = \phi_{r-ref}$ and $\phi_{rq} = 0$. The system equations of the DSAG after the orientation are given as follows (Merabet et al., 2011):

$$T_{em-ref} = p\frac{l_m}{(l_m + l_r)}(i_{sq1} + i_{sq2})\phi_{r-ref} \tag{13}$$

$$\Omega_{gl-ref} = \frac{r_r l_m}{(l_m + l_r)} \frac{(\mathrm{i}_{sq1} + \mathrm{i}_{sq2})}{\phi_{r-ref}} \tag{14}$$

$$\phi_{r-ref} = l_m (\mathrm{i}_{sd1} + \mathrm{i}_{sd2}) \tag{15}$$

Also the system (12) of the IM becomes as follow (Davigny, 2007):

$$\frac{d}{dt}\begin{pmatrix} \phi_{rd-fess} \\ i_{sd-fess} \\ i_{sq-fess} \end{pmatrix} = \begin{pmatrix} \frac{-R_r}{L_r} & \frac{MR_r}{L_r} & 0 \\ \frac{MR_r}{\sigma L_s L_r^2} & \frac{-R_{sr}}{\sigma L_s} & \omega_{fess} \\ \frac{-Mp\Omega_{fess}}{\sigma L_s L_r} & -\omega_{fess} & \frac{-R_{sr}}{\sigma L_s} \end{pmatrix} \begin{pmatrix} \phi_{rd-fess} \\ i_{sd-fess} \\ i_{sq-fess} \end{pmatrix} + \begin{pmatrix} 0 & 0 \\ 0 & 0 \\ \frac{1}{\sigma L_s} & 0 \\ 0 & \frac{1}{\sigma L_s} \end{pmatrix} \begin{pmatrix} v_{rd-fess} \\ v_{rq-fess} \\ 0 \\ 0 \end{pmatrix} \tag{16}$$

$$\omega_{fess} = p\Omega_{fess} + \frac{MR_r}{L_r} \frac{i_{sq-ref}}{\phi_{fess-ref}} \tag{17}$$

4. Synergetic control theory applied to the DSAG

4.1. Synergetic control theory

Synergetic control is an approach that combines many analytical methods for controlling, primarily nonlinear systems. The controller design process begins with the selection of a macro-variable, which is a linear function of the system variables. The goal of the control strategy is to keep the trajectories on the surface $\psi(\mathrm{x}) = 0$ and to have them advance exponentially away from the initial condition in the direction of the latter. Any nonlinear dynamical system of dimension n can be described as follows (Kolesnikov et al., 2000):

$$\dot{X} = f(\mathrm{x}, \mathrm{u}, \mathrm{t}) \tag{18}$$

x represents the system state, u represents the control, and t represents the time.

Starting with the state variables, a macro-variable is defined as

$$\Psi = \psi(\mathrm{x}, \mathrm{t}) \tag{19}$$

with $\psi(\mathrm{x})$ being a function defined by the user.

The system is forced to operate on the manifold and arrive at the desired state, and the macro-variable equals zero.

$$T\dot{\psi} + \psi = 0 \tag{20}$$

with: $T > 0$, where T is a constant time coefficient

By substituting (18) in (20) the control law can be obatined as follows

$$u = g(\mathrm{x}, \psi(\mathrm{x}, \mathrm{t}), \mathrm{T}) \tag{21}$$

4.2. Design of synergetic controller applied to DSAG

The control law can be obatined for a state function with Ω_r and ϕ_r which provides the necessary reference values Ω_{r-ref} and the reference flux ϕ_{r-ref}, the following equation can be used to describe the macro-variable:

$$\psi = k_1 x_1 + k_2 x_2 + k_3 \int x_1 dt \tag{22}$$

where: k_1, k_2 and k_3 are the synergetic controller parameters, $x_1 = \Omega_{r-ref} - \Omega_r$ and $x_2 = \phi_{r-ref} - \phi_r$

$$T\dot{\psi} + \psi = 0 \text{, with } T > 0 \tag{23}$$

By replacing $\dot{\psi}$ and ψ with their expressions, we obtain

$$T(k_1\dot{x}_1 + k_2\dot{x}_2 + k_3 x_1) + k_1 x_1 + k_2 x_2 + k_3 \int x_1 dt = 0 \tag{24}$$

By substitution, the control law is obtained

$$T_{em-ref} = \frac{J}{Tk_1}\left[(k_1(\Omega_{r-ref} - \Omega_r) + k_2(\phi_{r-ref} - \phi_r) + k_3\int x_1 dt) - (\frac{r_r}{l_r + l_m}\phi_r + (\iota_{sd1} + \iota_{sd2})(\frac{r_r l_m}{l_r + l_m}))Tk_2 + \Omega Tk_3\right] + T_L + k_f\Omega_r \tag{25}$$

5. Optimization of the synergetic controller by PSO algorithm

One of the best optimization techniques is the particle swarm optimization technique, which is superior to other optimization techniques due to its simplicity of implementation, robustness, and fast response. These factors led us to the use of the PSO method in this paper for tuning the parameters of the synergetic controller by looking for ideal values to reduce the error to the absolute minimum or zero. Figure 6 shows a diagram for the synergetic approach optimized by PSO algorithm. The particle swarm optimization begins with setting the positions and velocities of all particles at random inside a predetermined range (Abdolrasol et al., 2022)

$$\mathrm{v}_i(\mathrm{t}+1) = w \cdot \mathrm{v}_i(\mathrm{t}) + \varphi_1 r_1(t) \cdot (p_{bi}(\mathrm{t}) - \mathrm{x}_i(\mathrm{t})) + \varphi_2 r_2(t) \cdot (p_{gi}(\mathrm{t}) - \mathrm{x}_i(\mathrm{t})) \tag{26}$$

$$\mathrm{x}_i(\mathrm{t}+1) = \mathrm{x}_i(\mathrm{t}) + \mathrm{v}_i(\mathrm{t}) \tag{27}$$

Where $\mathrm{x}_i(\mathrm{t})$ and $\mathrm{v}_i(\mathrm{t})$ are the position and the velocity of particle i, respectively; the optimum position is p_{bi} while the optimal swarm position is p_{gi}; φ1 and φ2 are two accelerations that affect the relative weighting of linked terms; r_1 and r_2 are random parameters with values between [0,1]; and the inertiel weight W is chosen as a middle ground for the ability of the swarm to explore locally and globally.

In control engineering, preferred performance indices include the inetegral square error (ISE), through which the fitness function of the PSO can be obtained

$$ISE = \int_0^\infty e^2(t)dt \tag{28}$$

If we reach the maximum number of iterations, the algorithm stops and the optimized parameters shall be obtained. Otherwise, give back to the next iteration.

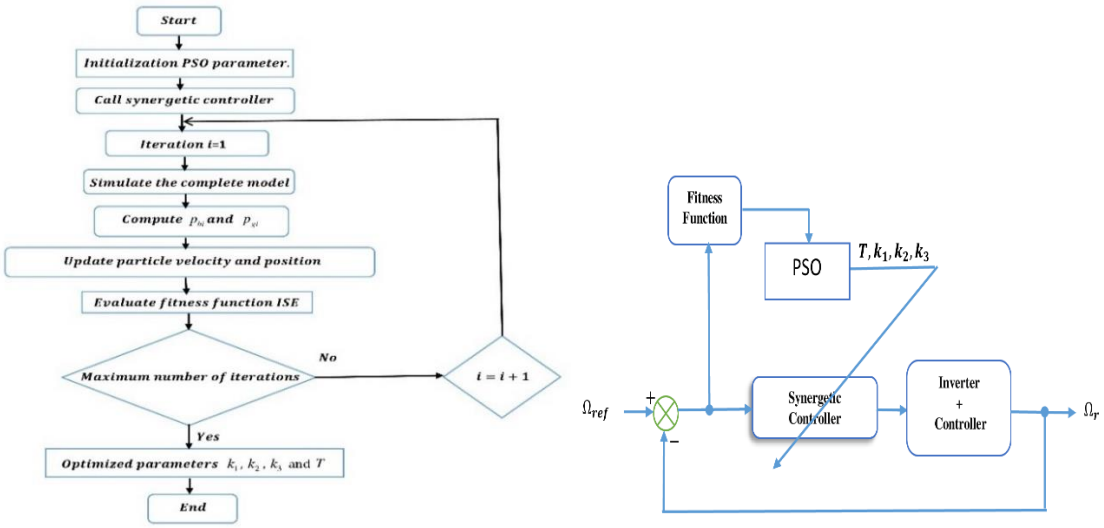

Figure 6. Optimization of the SC by the PSO Algorithm

6. Fuzzy design of the flywheel energy storage unit

To ensure the stability of the flywheel energy storage unit and improve its performance, a fuzzy logic algorithm was proposed, which is depicted in Figure 7. On the one hand, the flux of the machine was regulated to match its reference flux which calculated by

$$\begin{cases} \phi_{fess-ref} = \phi_{n-fess} & if \quad |\Omega_{fess}| \le \Omega_{rated} \\ \phi_{fess-ref} = \dfrac{\phi_{n-fess}\Omega_{rated}}{|\Omega_{fess}|} & if \quad |\Omega_{fess}| > \Omega_{rated} \end{cases} \tag{29}$$

On the other hand, the velocity of the asynchronous machine was regulated to match its reference velocity which was determined by equation (10).

The inputs of the Fuzzy controller are the error (e) and the change in the error Δe, and the output is the electromagnetic torque T_{em-ref} and for the flux controller, the output is the direct current i_{sd-ref}. The knowledge base, inference, defuzzification, and fuzzification interface make up the fuzzy controller (Zadeh, 1983). The gain k, k_e and $k_{\Delta e}$ are the parameters of the algorithm.

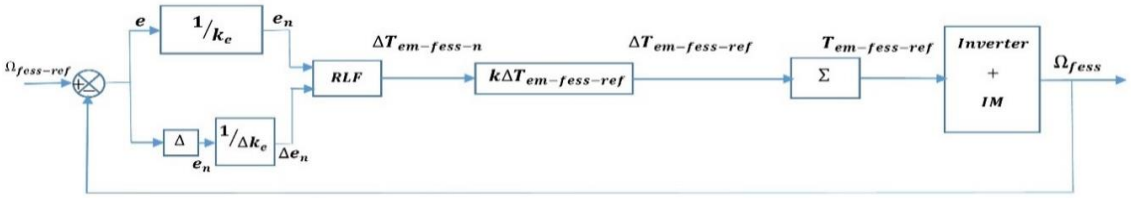

Figure 7. Fuzzy controller of FESS speed and flux

Each input and output fuzzy set has five typical triangle-type membership functions in the fuzzy controller. The following linguistic set has been (Kouzi et al., 2004): negative big (NB), negative small (NS), zero (EZ), positive small (PS), and positive big (PB).

The input errors are:

$$e_{\Omega}(k) = \Omega_{fess-ref} - \Omega_{fess} \tag{30}$$

$$e_{\phi}(k) = \phi_{fess-ref} - \phi_{fess} \tag{31}$$

The inference is the source of the fuzzy rules that enable the determination of the regulator output variable based on its input variables. Twenty five regulations are grouped together in this instance, as it is shown in the Table 1 (Rougab et al., 2021).

Table 1. Inference rules

Δe_n \ e_n	NB	NS	EZ	PS	PB
NB	NB	NB	NB	NS	EZ
NS	NB	NS	NS	EZ	PS
EZ	NB	NS	EZ	PS	PB
PS	NS	EZ	PS	PS	PB
PB	EZ	PS	PB	PB	PB

The outputs are determined by

$$T_{em-fess-ref} = T_{em-fess-ref} + K_{\Delta tem}\Delta_{tem} \tag{32}$$

$$\phi_{fess-ref} = \phi_{fess-ref} + K_{\Delta\phi}\Delta_{\phi} \tag{33}$$

7. Results and discussion

In order to evaluate the performance of the proposed system, two tests were performed in Matlab/Simulink. The simulation performed for a time period of one minute. The variable wind speed is shown in Figure 8.

7.1. First test: Simulation of the wind power conversion system without FESS

The model of the WPCS based on DSAG connected to the grid through the DC bus link is simulated with the condition: reactive power equal to zero $Q_{g-ref} = 0$ and $U_{dc-ref} = 1.131$ kV. The parameters of DSAG and of the wind turbine are listed in Table 2. It can be seen from the Figure 9 that the voltage U_{dc} was maintained at a constant value of 1.131 kV as its reference.

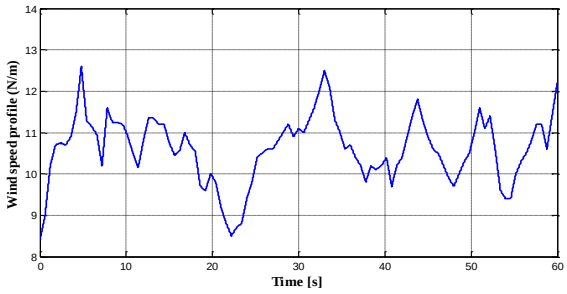

Figure 8. Wind speed

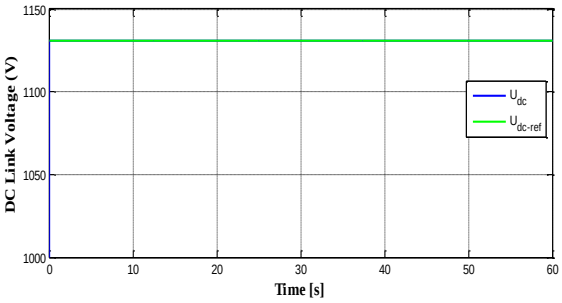

Figure 9. DC bus link voltage

The analysed system was greatly improved by the optimal synergetic control of the DSAG, as it is highlighted by the very quick reaction of the DSAG velocity as it is shown in Figures 10 and 11, with brief settling time of less than 1.10^{-3} s, and the velocity curve that exactly matches its reference.

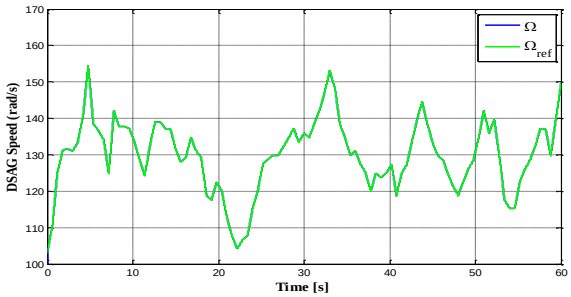

Figure 10. DSAG speed

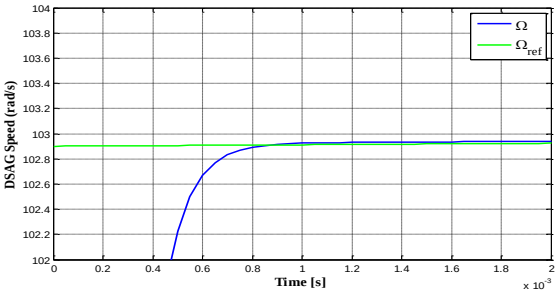

Figure 11. Zoom in DSAG speed

In Figures 12 and 13, it can be clearly seen that the reactive power of the wind generator is between 0.2 and 0.7 MW while it is zero on the grid side. It can also be noticed that the active powers of the wind generator and the grid have the same curve and are in a fluctuating state, which is due to the nature of the wind.

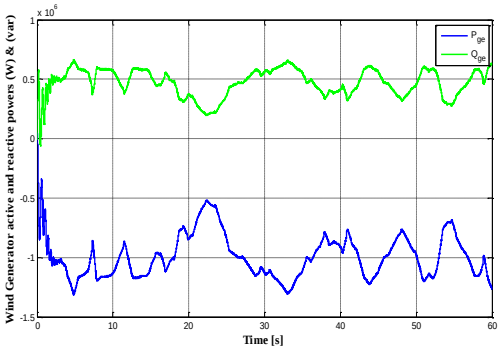

Figure 12. Wind generator powers

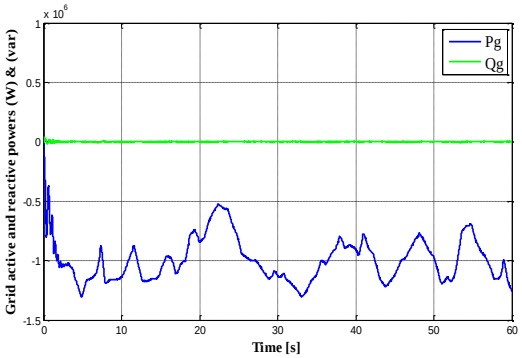

Figure 13. Grid side Powers

7.2. Second test: Integration of the FESS in the wind power conversion system

After evaluating the performance of the optimized synergetic control of the DSAG wind generator, the Flywheel energy storage system was integrated based on the IM in the analysed system to extract a constant power delivered to the grid from the wind generator equal to 1MW. The following figures show the simulation results.

Figure 14 shows that the active power of the grid side changed when the FESS was integrated and it became almost constant after it was variable and herein lies the importance of Fess. Figure 15 shows the grid side voltage and current, it is apparent that they are in opposing phases, indicating that the power is generated continuously.

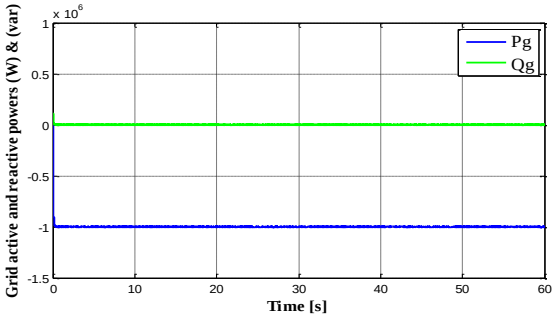

Figure 14. Grid powers after the integration of FESS

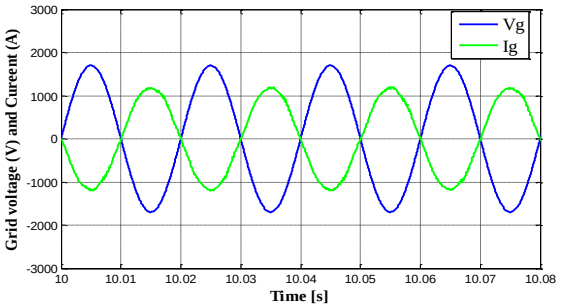

Figure 15. Grid current and voltage

Figure 16 shows the speed of Fuzzy Fess, which rises when Fess stores energy and falls when it feeds energy to the grid, it can also be noted that it follows its reference perfectly. Figure 17 demonstrates that the Fess machine functions both as a motor and a generator by showing how the active power changes between the positive and negative cases. The difference between the active power of the wind generator P_{ge} and the active power required P_{reg} is stored in the FESS, if there is a deficit, the power kept in the FESS will make up for that deficiency.

Figure 18 displays the electromagnetic torque of the Fess machine and its reference; evidently, the torque is positive during the storage while it is negative during the energy restitution phase. Figure 19 displays the two parts of the rotor flux of the Fess electrical machine, the quadratic flux of the rotor is zero, and the direct flux follows its reference perfectly, this is a result of the vector control.

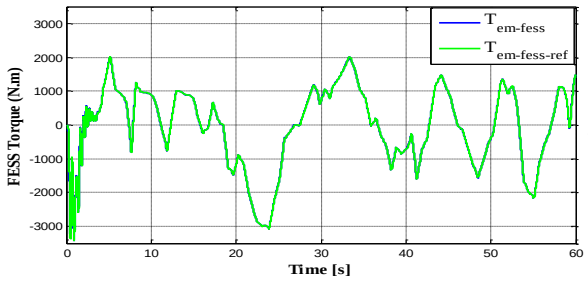

Figure 16. FESS mechanical speed

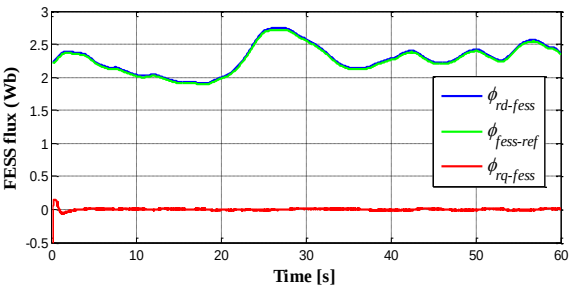

Figure 17. FESS active

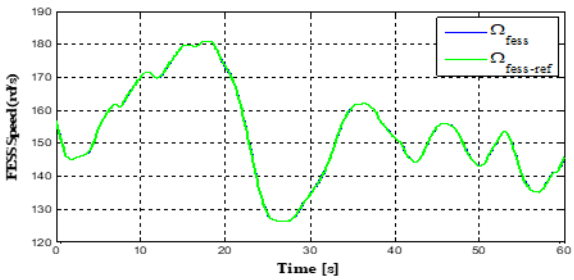

Figure 18. FESS electromagnetic torque

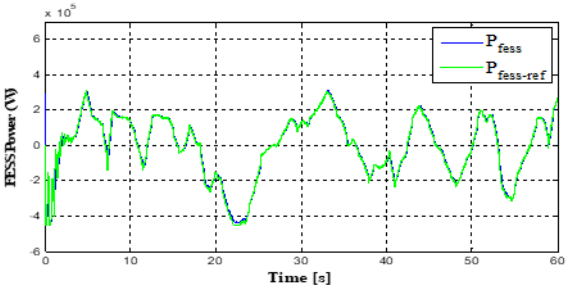

Figure 19. Fess flux

The Fess machine voltage and current curves are shown in Figure 20, while Figure 21 shows their zoom; between 8 and 8.08s it can be seen that the current and voltage have the same sign, so their product gives a positive sign power, in this case the IM acts as a motor by pushing the flywheel. While they are in phase opposition between 11.5 and 11.58s, the IM functions as a generator driven by the flywheel.

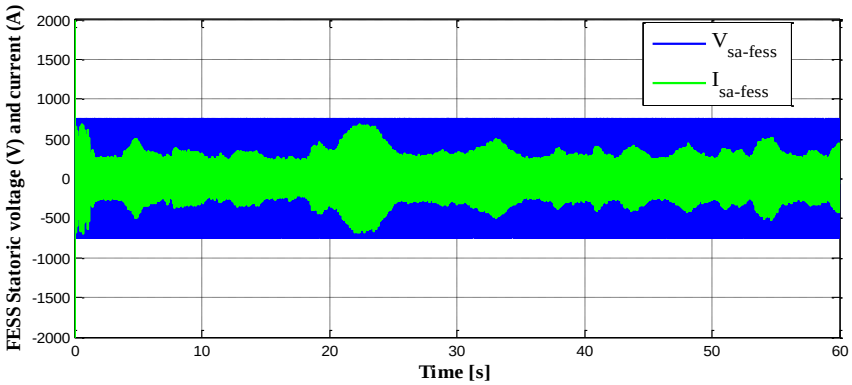

Figure 20. FESS stator voltage and current

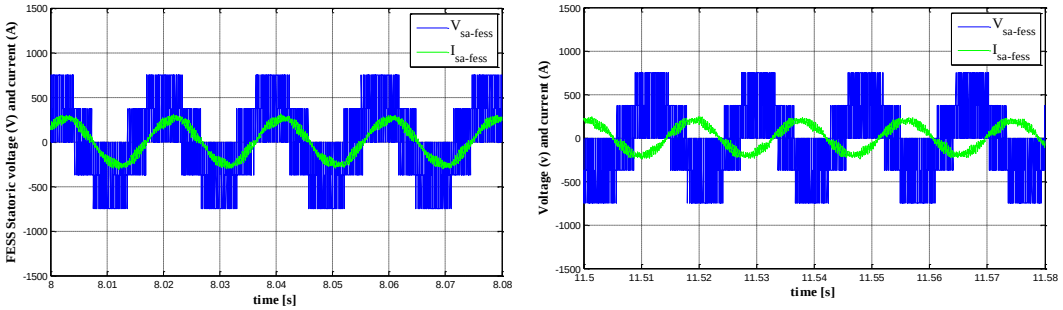

Figure 21. Zoom in Fess stator voltage and current

8. Conclusion

This paper provided a comprehensive model for the use of a wind turbine to produce electrical energy, and the flywheel energy storage unit was analysed, which is a great solution for helping wind turbines contribute to an electrical network. The dual-star asynchronous machine is connected to the wind turbine via the gearbox and it provided efficient and effective energy. Moreover, a synergetic controller was proposed, enabled the analysed system to reach a good performance with a very fast response of the generator speed. Furthermore, this analysis on the artificial intelligence, on the one hand, the parameters of the synergetic controller have been optimized by means of the particle swarm optimization algorithm, and on the other hand, the flywheel energy storage was controlled by the fuzzy logic algorithm.

Table 2. Parameters

Type	*Symbol and Value*
DSAG	V_{rated}=400 V, f = 50 Hz, 2 pole pairs, stator resistances $r_{s1} = r_{s2} = 0.008X$, rotor resistance $r_r = 0.008X$ stator inductances $l_{s1} = l_{s2} = 0.134$ mH, mutual inductance $l_m = 0.0045$ H, rotor resistance $r_r = 0.007\ X$, rotor inductance $l_r = 0.0067$ mH, inertia J=100 kg m^2, friction $K_f =$ 2.5 NmS/rd.
IM	400 V, 2 pole pairs, stator and rotor resistances $R_s = R_r = 0.0171\Omega$, stator and rotor inductances $L_s = L_r = 0.0173$ H, mutual inductance M=0.0135 H, inertia J_{fess}=250 kg m^2, friction $f_{fess} = 250$ NmS/rd.
Turbine	hub height is 85, G = 90, the radius R=35 m, 3 blades.

List of symbols

DSAG

T_{em} and T_L	Electromagnetic torque of the DSAG and the load
Ω_{gl-ref}	Slip speed
ϕ_{rd} and ϕ_{rq}	Components of rotor winding flux
ϕ_{r-ref}	Rotor flux reference
i_{sd1}, i_{sd2}, i_{sq1} and i_{sq2}	Components of stator currents
v_{sd1}, v_{sd2}, v_{sq1} and v_{sq2}	Components of stator voltages
p	Number of pair poles
ω_s	Synchronous reference frame speed

FESS

$T_{em-fess}$	Electromagnetic torque
$\phi_{rd-fess}$ and $\phi_{rq-fess}$	Components of rotor winding flux of FESS
$v_{rd-fess}$ and $v_{rq-fess}$	Components of stator voltages
$i_{sd-fess}$ and $i_{sq-fess}$	Components of stator currents
ω_{fess}	Synchronous reference frame speed
Ω_{rated}	Nominal mechanical speed
P_{rated}	Nominal power

REFERENCES

1. Abdolrasol, M. G. M., Hannan, M. A., Suhail Hussain, S. M., & Ustun,T. S. (2022). Optimal PI Controller Based PSO Optimization for PV Inverter Using SPWM Techniques, In the 8th International Conference on Power and Energy Systems Engineering, *Energy Reports*, 8, 1003-1011. DOI: https://doi.org/10.1016/j.egyr.2021.11.180.
2. Amimeur, H. (2012). *Contribution au Controle de la Machine Asynchrone Double Etoile*, PhD Thesis, University of Batna. Algeria.
3. Amimeur, H., Aouzellag, D., Abdessemed, R. & Ghedamsi, K. (2012). Sliding mode control of a dual-stator induction generator for wind energy conversion systems. *International Journal of Electrical Power and Energy Systems*. https://doi.org/10.1016/j.ijepes.2012.03.024.
4. Chen, L. & Fang, K-L. (2003). A novel direct torque control for dual-three-phase induction motor. In *Proceedings of the second international conference on machine learning and cybernetics*, DOI: 10.1109/ICMLC.2003.1259602.
5. Cimuca, G. (2005). *Système inertiel de stockage d'énergie associé à des générateurs éoliens,* Ph.D. thesis, National School of Arts and Crafts, Center of Lille, France.
6. Cimuca, G., Berban, S., Radulescu, M. M., Saudemont, C. & Robyns, B. (2010). Design and Control Strategies of an Induction-Machine-Based Flywheel Energy Storage System Associated to a Variable-Speed Wind Generator. *IEEE Transactions on Energy Conversion*, 25(2), 525-534. IEEE. DOI: 10.1109/TEC.2010.2045925.
7. Davigny, A. (2007). *Participation aux Services systèmes de fermes d'éoliennes à vitesse variable intégrant du stockage inertiel d'énergie.* Ph.D. Thesis, University of Lille France.
8. Davoudi, A., Bazzi, A. M., Chapman, P. L. (2008). Application of synergetic control theory to non-sinusoidal PMSMs via multiple reference frame theory. In *34th Annual Conference if IEEE Industrial Electronics*, (pp. 2794-2799) IEEE. https://doi.org/10.1109/IECON. 2008.4758401.
9. El Aimani, S. (2004). *Modelisation de différentes technologies d'éolienne intégrées dans un réseau de moyen tension*, Ph.D. Thesis University of Toulouse, France.
10. Gergaud, O., Multon, B & Ben Ahmed, H. (2001). Modélisation d'une chaîne de conversion éolienne de petite puissance. *L'Electrotechnique du Futur 2001*, (pp. 17-22), Nancy, November.

11. Guermit, H. & Kouzi, K. (2018). Investigate the Performance of an Optimized Synergetic Control Approach of Dual Star Induction Motor Fed by Photovoltaic Generator with Fuzzy MPPT. In *International Conference in Artificial Intelligence in Renewable Energetic Systems*, (pp. 297-310). https://doi.org/10.1007/978-3-030-04789-4_33.
12. Hamidat, M., & Kouzi, K. (2022). Performances of vector control of a Brushless Dual-Fed Induction Generator Incorporated in a wind energy conversion system with OTC-MPPT. *Romanian Journal of Information Technology and Automatic Control*, 32(2), 7-19. DOI: https://doi.org/10.33436/v32i2y202201.
13. Jia, Y., Wu, Z., Bao, M., Zhang, J., Yang, P., Zhang, Z. (2022). *Control strategy of MW flywheel energy storage system based on a six-phase permanent magnet synchronous motor*, Energy Reports, https://doi.org/10.1016/j.egyr.2022.09.048.
14. Kennedy, J. & Elberhart, R. (1995). Particle swarm optimization. In *Proceedings of the IEEE International Conference on Neural Network*, (pp. 1942-1948), Morgan Kaufman Publishers, Burlington.
15. Kolesnikov, A., Veselov, G., Popov, A., Kolesnikov, A., Kuzmenko, A., Dougal, R.A., & Kondratiev, L. (2000). A synergetic approach to the modeling of power electronic systems. In *Proceedings of the 7th workshop on Computers in Power Electronics (COMPEL)*, vol. 1, (pp. 259-262). DOI: 10.1109/CIPE.2000.904726.
16. Kouzi, K., Mokrani, L. & Nait, M.S. (2004). High performances of fuzzy self-tuning scaling factor of PI fuzzy logic controller based on direct vector control for induction motor drive without flux measurements. In *Proceedings of IEEE International Conference on Industrial Technology*, 8-10 December 2004: Hammamet Tunisia, (pp. 1106-1111).
17. Leclerq, L. (2004). *Apport du stockage inertiel associé à des éoliennes dans un réseau électrique en vue d'assurer des services systèmes*, Ph.D. Thesis, Lillle University.
18. Merabet, E., Amimeur, H., Hamoudi, F & Abdessemed, R. (2011). Self-tuning fuzzy logic Controller for a dual star induction machine. *Journal of Electrical Engineering & Technology*, 6(1), 133-138.
19. Mousavi, S. M. G., Faraji, F., Majazi, A. & Al-Haddad, K. (2017). A comprehensive review of Flywheel Energy Storage System. *Renewable and Sustainable Energy Reviews*, 67, 477-490, DOI: https://doi.org/10.1016/j.rser.2016.09.060.
20. Rougab, I., Cheknane, A. & Abouchabana, N. (2021). Study and simulation of MPPT techniques to control a stand-alone photovoltaic system. *Romanian Journal of Information Technology and Automatic Control*, 31(4), 109-122. DOI: https://doi.org/10.33436/v31i4y202109.
21. Zadeh, L. A. (1983). The Role of Fuzzy Logic in the Management of Uncertainty in Expert Systems. *Fuzzy Sets and Systems*, 11(1-3), 199-227. https://doi.org/10.1016/S0165-0114(83)80081-5.

Djamel DERKOUCHE was born in Djamaa, Algeria. He obtained a Bachelor's Degree in Electro-Mechanical Engineering from the University of Djelfa in 2010 and a Master's Degree in 2016, in the same specialty. Currently, he is a Ph.D. student at the Electrical Control Department, at the University of Laghouat in Algeria. His research interests focus on renewable energy systems and control of electric vehicles.

Katia KOUZI was born in Algeria. She obtained her Bachelor's Degree in 1998 and, later, her Master's Degree in Electrical Engineering, in 2002. She received her Ph.D. Degree in Electrical and Computer Engineering from the University of Batna, in 2008. Her research interests focus on Advanced Control of AC Drives, including Vector, Sensorless and Intelligent Artificial Control, Electric vehicles (EVs) Control, Renewable Energy Control Systems, Management and Storage Systems. She is a researcher at the Laboratoire Matériaux, Systèmes Énergétiques, Energies Renouvelables et Gestion de l'Énergie (LMSEERGE), as well as a full-time professor at the Electrical Engineering Institute of the University of Laghouat in Algeria.